Local distortions and spin parameters of Gd^{3+} in some orthorhombic CaF_2 complexes

Local distortions and spin parameters of Gd³⁺ in some orthorhombic CaF₂ complexes

Y Y Yeung

Department of Applied Physics, Hong Kong Polytechnic, Hong Kong

Abstract. The ionic positions of Gd^{3+} at orthorhombic sites in CaF_2 with a nearby charge-compensating M^+ ion (M = Li, Na, K, Rb and Cs) are calculated from a reliable lattice relaxation model. The results are then employed in superposition model analyses of the corresponding spin parameters of the ground state $4f^7\ {}^8S_{7/2}$ splitting of the Gd^{3+} ion available in the literature. The superposition model analyses indicate that the spin parameters can best be described in terms of some intrinsic parameters which follow a parabolic dependence on the ligand distances in addition to the conventional power-law form, and hence also assert the cancelling nature of various physical mechanisms contributing to the ground state splitting of Gd^{3+}.

1. Introduction

For a number of years the zero-field splitting of orthorhombic Gd^{3+}–M^+ complexes (M = Li, Na, K, Rb and Cs) in CaF_2 has been an interesting problem for the EPR theorists and experimentalists (see, e.g. Edgar and Newman 1975, Lefferts *et al* 1978, Bijvank *et al* 1977, 1980a, b) who have made a systematic tabulation of the spin parameters for the $^8S_{7/2}$ ground state splitting of the Gd^{3+} ion. Geometrically, each system of this complex consists of a local charge-compensating M^+ ion located at a $[\bar{1}10]$ position with respect to the Gd^{3+} ion, both being doped at the Ca^{2+} sites such that the site symmetry of Gd^{3+} is lowered from O_h to C_{2v} (see figure 1). It is generally expected that the dramatic variations of the spin parameters B_n^m for various M^+ complexes are closely related to the non-cubic lattice distortions induced by the M^+ ions. Hence, several previous workers have attempted various approaches such as the superposition model (Edgar and Newman 1975) and local distortion calculation (Bijvank and Hartog 1980b) to analyse and to correlate those spin parameters with the local distortions. However, their results are still rather unsatisfactory (as we shall see below), allowing much room for improvement.

In the superposition model, the spin parameters B_n^m are separated into the radial and angular parts as follows:

$$B_n^m = \sum_i \bar{B}_n(R_i) K_n^m(\theta_i \phi_i) \tag{1}$$

where $R_i \theta_i \phi_i$ are the spherical coordinates of the ith ligand and their angular variations are contained in the coordination functions $K_n^m(\theta \phi)$ tabulated by Newman
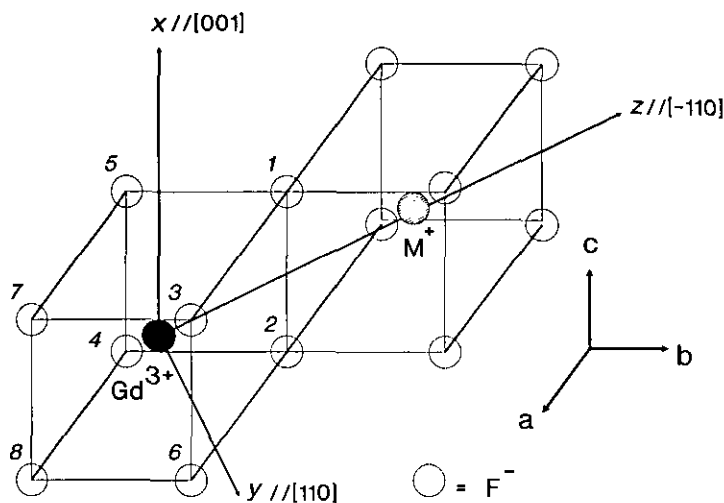
Figure 1. The undistorted configuration of the orthorhombic Gd^{3+}: M^+: CaF_2 complex. The coordinated F^- ligands of Gd^{3+} are labelled 1 to 8. The xyz coordinate axes are centred at the Gd^{3+} ion and their orientation is given in terms of the crystal axes a, b and c.

and Urban (1975). For the contributions to the radial intrinsic parameters $\bar{B}_n$, there exist a number of different physical mechanisms (see Newman and Urban (1975) for earlier references) such as the one-particle crystal field (CF) (including electrostatic, overlap and covalency contributions), the quadratic CF (Siu 1990), the relativistic CF, the dynamical relativistic CF (Pastusiak 1984), the two-particle correlation CF (e.g. spin-correlated CF (Yeung and Newman 1986), orbitally correlated CF (Yeung and Newman 1987)) and the Pryce (1950) mechanism etc. which make dissimilar (in both sign and magnitude) contributions to $\bar{B}_n$. Some preliminary calculations for the rank 2 parameter $\bar{B}_2$ did indicate that the contributions from the CF and relativistic CF are opposite in sign to those from the correlation CF and their distance variations should theoretically be different. Hence, it is proposed that the overall distance variation of $\bar{B}_n$ is likely to follow a double-power-law form:

$$\bar{B}_n(R) = \bar{B}'_n (R_0/R)^{t'_n} + \bar{B}''_n (R_0/R)^{t''_n} \qquad (2)$$

which will yield a U-shaped curve near R_0 (see figure 9 of Newman and Urban 1975) as a consequence of the various cancelling contributions. Amongst the current applications of the superposition model, little effort has been devoted to the accurate determination of local ligand positions R, θ, ϕ which should be different from the perfect host positions due to the impurity-ion-induced local distortion. As a result, it is normally impossible to obtain all the contributing parameters for the $\bar{B}_n$ in (2), to wit, $\bar{B}'_{n'}$, $\bar{B}''_{n'}$, t'_n and t''_n from the limited empirical spin parameters, and so almost all previous work has assumed, for simplicity and practicality, a single power-law form for the intrinsic parameters

$$\bar{B}_n(R) = \bar{B}_n(R_0)(R_0/R)^{t_n} \qquad (3)$$

to be valid for all range of ligand distance R. Unfortunately, the empirical $\bar{B}_n(R_0)$ of Gd^{3+} derived from this power-law form for various systems (without proper allowance

for local distortion) of the same ligand type are found to be at variance in both sign and magnitude (see, e.g., table 4 of Newman 1975), raising the question of *transferability* and *superposability* of individual ligand contributions to overall zero-field splitting (Novak and Vosika 1983).

On the other hand, Yeung and co-workers (e.g. Yeung 1988, Yeung and Newman 1988, Choy and Yeung 1990) have recently developed a lattice relaxation model for calculating the positions of ligands (including local distortion effect) surrounding a point defect based on the Kanzaki (1957) 'lattice statics' approach which was originally introduced to calculate the local atomic displacements around a vacancy in solid argon. In our previous relaxation model for a defect system consisting of a substitutional Eu^{2+} ion plus a local charge-compensating vacancy in the rocksalt lattice, the shell model (Cochran 1971) was employed to describe the dynamical matrix of the host ionic lattice and hybridized with the lattice statics method which deals with the additional long-range coulombic interactions arising from the charged defects as well as the Kanzaki's short-range repulsive forces. The calculated local distortions for Eu^{2+} in a group of 12 alkali halides were subsequently used to carry out a superposition model analysis of the spin-Hamiltonian parameters of Eu^{2+}. The fits (Yeung and Newman 1988) turned out to be much better than those obtained by other workers and the values are consistent with those obtained for Eu^{2+} and Gd^{3+} in other systems, providing a significant extension of our understanding of the properties of $4f^7$ ground S-state spin parameters. Further applications had been made to calculate the local distortion induced by the Gd^{3+} ion doped at cubic sites in various fluorites such as CdF_2, CaF_2, SrF_2, PbF_2 and BaF_2 (Yeung 1988). The calculated ligand distances are found to be almost entirely consistent with those derived from the superhyperfine and spin parameters of Gd^{3+}. Hence it is plausible to extend this method to calculate the displacements of all ions surrounding the Gd^{3+} ion in the present orthorhombic CaF_2 complexes and to check the goodness of the results by analysing the spin parameters for the ground state splitting of Gd^{3+} using the superposition model.

2. Local distortions around Gd³⁺–M⁺ complexes in CaF₂

2.1. Theory of calculations

When a Gd^{3+} ion is doped at the Ca^{2+} site in the host CaF_2 crystal, lattice distortions will occur naturally due to the differences in the short-range repulsive potential and ionic charges between the host cation and the substituent. In our lattice relaxation model, the effect of a point defect is replaced by a set of external 'Kanzaki' forces which can characterize all the defect-induced properties. Furthermore, the ionic displacements $\xi(l\kappa)$ for the κ-type ion of the lth unit cell in the defect crystal, which is essentially a perfect lattice modulated by some external Kanzaki forces $F(l\kappa)$, are treated using the discrete atomistic basis. The change $\Delta\Phi$ in the potential energy between the defect and perfect crystals is to be minimized under the harmonic approximation. The equilibrium equations of atomic displacements, to wit, $\partial\Delta\Phi/\partial\xi(l\kappa) = 0$, are then decoupled into matrix equations of very small size (9×9 for the CaF_2 lattice) in the reciprocal lattice k-space by Fourier transform. Hence, the displacements $u(k)$ in the reciprocal lattice space are obtainable from (see Yeung and Newman (1988) for details of derivation)

$$\mathbf{M}u = e(\mathbf{Z} - \mathbf{A}_{CS}\mathbf{A}_{SS}^{-1}\mathbf{Y})E^{(0)} + (\mathbf{I} - \mathbf{A}_{CS}\mathbf{A}_{SS}^{-1})\bar{F} \qquad (4)$$

where $M \equiv A_{CC} - A_{CS}A_{SS}^{-1}A_{SC}$ is the usual dynamical matrix and its detailed components for CaF_2 crystal are given explicitly by Elcombe and Pryor (1970). Briefly, the A matrices represent the quadratic potential energy for the shell model (Cochran 1971) description of the interactions between ionic cores C and shells S in the crystal. The matrices Z and Y denote the ionic charges for the core and shell respectively. The generalized Kanzaki forces F consist of the long-range extra electric field $E^{(0)}$ generated by the charge difference between the defect and host lattice ions and the defect-induced local force $\bar{F}$ which is composed of the short-range repulsive part $\bar{F}^R$ and a part from some higher-order coulombic contribution $\bar{F}^C$. Due to the cubic site symmetry of Gd^{3+} doped at Ca^{2+} site, we may assume the nearest-neighbour interaction to be radial in direction so that there is only one independent force component $\bar{F}$ for $\bar{F}(l\kappa) = \bar{F}\hat{r}(l\kappa)$, and one independent displacement component ξ for $\xi(l\kappa) = \xi\hat{r}(l\kappa)$ for interaction with an anion F^- ligand initially at $r_F = r(l\kappa)$. Then, in terms of the short-range potential $v(r)$ (with subscript D for a defect at a κ'-type cation site), we have

$$\bar{F}^R = -v'_D(r_F + \xi) + v'(r_F) + \xi v''(r_F) \tag{5}$$

$$\bar{F}^C \approx -Z_\kappa (Z^D_{\kappa'} - Z_{\kappa'})e^2(2/r_F^3)\xi. \tag{6}$$

Putting $\bar{F} = \bar{F}^R + \bar{F}^C$ into equation (4), we may obtain the ionic displacements in direct lattice space using the following equation

$$\xi(l\kappa) = \frac{1}{N}\sum_k u(k)\exp(-ik \cdot r(l\kappa)) \tag{7}$$

where N is the total number of wavevectors k taken in the inverse Fourier transform. The nearest-neighbour displacement ξ can furthermore be decomposed into three components.

$$\xi = \xi^E + \xi^R(\bar{F}^R) + \xi^C(\bar{F}^C) \tag{8}$$

where ξ^E corresponds to the contribution arising from the long-range coulombic term $E^{(0)}$ of (4). Here ξ^R and ξ^C are respectively linear functions of $\bar{F}^R$ and $\bar{F}^C$ which are themselves functions of ξ. Hence, the unknowns ξ, $\bar{F}^R$ and $\bar{F}^C$ in the set of equations (5), (6) and (8) have to be solved simultaneously by numerical methods.

In studying the local distortions for our Gd^{3+}-M^+ pair system, the origin (see figure 1) is taken at the Gd^{3+} site $r_{Gd} = 0$ and the alkali metal ion M^+ is located at site $r_M = (\bar{1}10)r_0$. We initially consider the ionic displacements induced by the Gd^{3+} and M^+ ions separately. By translational symmetry, we may again utilize equation (7) to find the alkali metal ion induced displacements ξ_M if we take the new coordinate frame with origin at r_M, i.e. $r(l\kappa) \rightarrow r(l\kappa) - r_M$. Also, we have to substitute v_D and $Z^D_{\kappa'}$ by v_M and $Z^M_{\kappa'}$, which are both different from those for the Gd^{3+} defect, so that the previous formalism can be applied to the M^+ system directly. Secondly, we should include the extra ionic displacements induced by the change in Gd^{3+}-M^+ interaction with respect to the perfect crystal (to wit, the change in their coulombic and short-range repulsive interactions). The corresponding effect can simply be expressed as an additional interaction force $F_I = F_I\hat{r}_M$, which replaces the short-range force $\bar{F}$ of (4). This new force F_I will consequently displace the Gd^{3+} and M^+ ions towards each other and hence induce some extra displacements ξ_I to other ions.

Overall, the resultant ionic displacements ξ are the direct sums of displacements induced by three sources, namely, the Gd^{3+} defect, the M^+ defect and the additional interaction between the two point defects. In other words

$$\xi = \xi_{Gd} + \xi_M + \xi_1 \tag{9}$$

where

$$\xi_{Gd,M,I} = \xi_{Gd,M,I}(F_{Gd,M,I}) \tag{9a}$$

$$\bar{F}_{Gd,M,I} = \bar{F}_{Gd,M,I}(\xi). \tag{9b}$$

All quantities in the above equations refer to direct lattice space and they are to be solved simultaneously. In practice, we may rewrite the force equation (9b) as

$$\bar{F}_{Gd,M,I} = \bar{F}_{Gd,M,I}(\xi_{Gd,M,I})$$

in the first approximation and then seek self-consistent results by iteration.

2.2. Results and discussions

In the present calculations, the force parameters for the lattice relaxation model (including those for the shell model of the lattice dynamical matrix) of the CaF_2 crystal are taken from Elcombe and Pryor (1970) and same as those used by Yeung (1988) while the interaction potential parameters of the Born–Mayer form for the M^+-F^- pairs are adopted from those tabulated by Bijvank and Hartog (1980b). The local displacements of the nearest- and next-nearest-neighbour ions of Gd^{3+} and M^+ in the above-mentioned five orthorhombic CaF_2 complexes have been calculated but the results are too lengthy to be fully presented here. Instead, only the shifts of a few ions in the $Gd^{3+} : K^+ : CaF_2$ complex are given in table 1 because they can be compared with some experimental data such as the ENDOR (Bijvank and Hartog 1980a) and the electron spin echo envelope modulation (ESEEM) measurement (Drogendijk et al 1987). Those results can also be compared with previous local distortion calculations by Bijvank and Hartog (1980b) who have followed Mott and Littleton's (1938) 'semi-discrete' approach in which only a very limited number of ions around the defects were treated as discrete entities and the remainder of the crystal was regarded as a dielectric continuum. This continuum approximation for most of the defect crystal is obviously less reliable than our present discrete atomistic (and harmonic approximation) approach for the whole crystal. Intrinsically, Mott and Littleton's approach possesses a mismatch problem for the displacements of ions lying at the interface between the discrete and continuum regions. In principle, the errors caused by the continuum approximation and mismatch problem can be reduced by taking a sufficiently large discrete region but this will necessitate a tremendous increase in computing time and memory. Hence, Bijvank and Hartog were able to consider only a rather small number of relaxing ions in the discrete region, namely, 24 and 44 for their methods A and B, respectively. From table 1, it is obvious that ours are quite consistent with the experimental data as well as the more accurate calculations (method B) by Bijvank and Hartog (1980b). It is noted that the ENDOR data are reliable only for more distant ligand positions whereas the ESEEM measurement for the change in $Gd^{3+}-K^+$ distance by Drogendijk et al (1987) clearly asserts the higher reliability of our relaxation model.

Table 1. Calculated shifts (in Å) of ions in Gd^{3+}: K^+: CaF_2 complex.

Ion (host lattice site)	Bijvank and Hartog (1980b)		Present calculation	Experiment
	Method A	Method B		
Gd^{3+} (000)	0.03	0.06	0.002	$<0.03^a$
f^- $(\frac{1}{2}\frac{1}{2}\frac{3}{2})$	0.05	0.02	0.02	$<0.05^a$
F^- $(\frac{1}{2}\frac{1}{2}\frac{3}{2})$	0.05	0.02	0.02	0.04^a
F^- $(\frac{1}{2}\frac{3}{2}\frac{1}{2})$	0.80	0.27	0.25	0.28^a
Fractional change in Gd^{3+}–K^+ distance				
	3.7%	2.7%	1.8%	$2.0 \pm 0.1\%^b$

[a] ENDOR data from Bijvank and Hartog (1980a).
[b] ESEEM measurement from Drognedijk *et al* (1987).

3. Superposition model analyses of spin parameters of Gd^{3+}

As suggested by Newman and Urban (1975), the superposition model analyses of the spin parameters of Gd^{3+} in various orthorhombic CaF_2 complexes using equation (1) should form another objective assessment on the accuracy of our calculated positions for the nearest ligands of Gd^{3+}. Before proceeding, the displaced ligand positions have to be expressed in polar coordinates with the origin of the xyz axes being located at the Gd^{3+} ion (see figure 1). Then, the calculated positions (R_i, θ_i, ϕ_i) for the eight nearest-neighbour F^- ligands of Gd^{3+} at cubic and orthorhombic sites in CaF_2 are given in table 2. From the C_{2v} site symmetry of Gd^{3+}, it is noted that $R_{2i} = R_{2i-1}$, $\theta_{2i} = \theta_{2i-1}$, $\phi_{2i} = \phi_{2i-1} + 180°$, $\phi_1 = \phi_7 = 0$, $R_5 = R_3$, $\theta_5 = \theta_3$, and $\phi_5 = 360° - \phi_3$. The extent of the local distortion can be seen from the comparison with the perfect host lattice values in which $R_i = 2.354$ Å, $\theta_1 = 35.26°$, $\theta_3 = 54.74°$ and $\theta_7 = 144.74°$. Putting those values of ligand polar coordinates into equation (1), it is tried to fit the experimental spin parameters (tabulated in table I of Lefferts *et al* 1978) for all the five M^+ complexes simultaneously to the intrinsic parameters $\bar{B}_n(R_i)$ of the form given by equation (3) as well as a new form which reads

$$\bar{B}_n(R_i) = \bar{B}'_n(R_0)(R_0/R_i)^{t_n} + \bar{B}''_n(R_0)((R_i - R_0)/R_0)^2. \quad (10)$$

The results for the rank $n = 2$ and 4 parameters are respectively summarized in tables 3 and 4 which also includes the fits using the ligand positions derived directly from Bijvank and Hartog's (1980b, method B) local distortion calculation. Note that the quality of fit χ defined in Cochran (1971) is minimized in each of the least-squares fit but it is equally well represented by the RMS deviations.

   Comparing fits (*a*) and (*c*) for the first term of equation (10) i.e. $\bar{B}''_n = 0$ which is equivalent to the conventional power-law form (3) for the distance dependence of the intrinsic parameter $\bar{B}_n(R)$, the RMS deviations in tables 3 and 4 clearly indicate that our calculated ligand positions are better than those of Bijvank and Hartog (1980b) in describing the spin parameters. For fits (*b*) and (*d*) in tables 3 and 4, we add the parabolic term of (10) with one additional free parameter $\bar{B}''_n$ for each rank n. From the relative changes in the RMS deviations between (*a*) and (*b*) for Bijvank and Hartog's ligand positions and between (*c*) and (*d*) for ours, we immediately see that the parabolic term in (10) does yield a very great improvement

Table 2. Calculated polar positions of the coordinated F^- ligands of Gd^{3+} in the cubic (Gd^{3+} only) and various orthorhombic (with charge-compensating M^+ ion) CaF_2 complexes. The coordinate frame and the ligand labels are defined in figure 1. The ligand distances R_i and angles θ_i and ϕ_i are given in units of Å and degrees, respectively.

Ligand polar coordinates	Gd^{3+} only	Gd^{3+} and charge-compensating M^+ ion				
		Li	Na	K	Rb	Cs
R_1	2.325	2.279	2.278	2.277	2.278	2.281
θ_1	35.264	38.61	39.49	41.36	42.27	44.10
R_3	2.325	2.375	2.381	2.394	2.401	2.413
θ_3	90.000	91.75	91.55	91.14	90.94	90.54
ϕ_3	54.736	55.36	55.49	55.77	55.91	56.18
R_7	2.325	2.382	2.372	2.352	2.342	2.322
θ_7	144.736	145.37	145.19	144.79	144.59	144.19

Table 3. Superposition model analyses of the rank-2 spin parameters (tabulated by Lefferts *et al* 1978) of the five Gd^{3+}: M^+: and CaF_2 complexes (M = Li, Na, K, Rb and Cs) using the calculated ligand positions from Bijvank and Hartog (1980b) and from the present work (see table 2). All parameters apart from t_2 and R_0 are in units of G ($1G = 9.300 \times 10^{-5}$ cm^{-1}). [X] means X is fixed in the fitting and values in parentheses indicate errors in the last figures.

		Experiment	Bijvank and Hartog (1980b)		Present calculation		
			(a)	(b)	(c)	(d)	(e)
Li$^+$	B_2^0	17.7(2)	−10.3	20.3	49.0	3.0	3.0
	B_2^2	−46.3(2)	−53.1	−35.6	5.2	−47.9	−47.9
Na$^+$	B_2^0	3.4(2)	5.3	31.6	68.2	34.8	34.8
	B_2^2	−30.0(2)	−19.5	−0.0	−0.93	−41.8	−41.8
K$^+$	B_2^0	83.6(2)	55.7	60.0	109.2	103.1	103.1
	B_2^2	−20.1(2)	−110.3	−102.9	−14.5	−25.9	−25.9
Rb$^+$	B_2^0	141.8(2)	119.5	144.8	129.3	136.8	136.8
	B_2^2	−11.9(2)	−16.4	16.4	−21.5	−16.3	−16.3
Cs$^+$	B_2^0	220.5(2)	141.3	154.6	169.5	204.6	204.6
	B_2^2	−4.0(2)	−72.2	−43.1	−35.9	7.2	7.2
$\bar{B}_2'$			−486(128)	−436(123)	−316(56)	−261(26)	−260(26)
$\bar{B}_2''/1000$			[0]	12(9)	[0]	−60(10)	−60(10)
R_0(Å)			[2.354]	[2.354]	[2.354]	[2.354]	2.348(2)
t_2			4.5(15)	6.8(26)	−0.72(64)	−2.2(5)	[-1]
RMS deviation			46.2	40.0	36.4	14.8	14.8

in the superposition model description of the spin parameters. It is remarked that the rank $n = 2$ spin parameters (table 3) can be used as a sensitive probe to measure the non-cubic displacements of the ligands surrounding the Gd^{3+} ion as their values are identically zero for Gd^{3+} at cubic site symmetry. In contrary, the rank 4 spin parameters (table 4) are less sensitive to local distortions because there are already some large values of non-zero cubic components, B_4^m (cubic) $\geqslant 10 B_4^m$ (non-cubic), overshadowing the minute crystal field effect due to non-cubic distortions. Although the conventional form has yielded a good fit for the rank 4 spin parameters of Gd^{3+} at cubic sites in various fluorite lattices (see Yeung (1988) for detailed references)

Table 4. Superposition model analyses of rank 4 spin parameters of the five Gd^{3+} : M^+ : CaF_2 complexes (see table 3 for details). All parameters except t_4 and R_0 are in units of G and $1G = 9.300 \times 10^{-5}$ cm^{-1}. $[X]$ means X is fixed in the fitting and values in parentheses indicate errors in the last figures.

			Bijvank and Hartog (1980b)		Present calculation		
		Experiment	(a)	(b)	(c)	(d)	(e)
Li$^+$	B_4^0	0.139(5)	0.165	0.167	0.193	0.168	0.168
	B_4^2	4.07(5)	4.09	4.02	3.98	4.01	4.01
	B_4^4	−2.85(5)	−2.86	−2.88	−3.01	−2.84	−2.84
Na$^+$	B_4^0	0.164(5)	0.180	0.183	0.189	0.168	0.168
	B_4^2	4.12(5)	4.07	4.02	3.98	4.00	4.00
	B_4^4	−2.95(5)	−2.94	−2.96	−3.01	−2.88	−2.88
K$^+$	B_4^0	0.185(5)	0.136	0.136	0.181	0.174	0.174
	B_4^2	3.97(5)	4.16	4.15	3.97	4.00	4.00
	B_4^4	−3.27(5)	−2.82	−2.83	−3.01	−2.99	−2.99
Rb$^+$	B_4^0	0.181(5)	0.175	0.180	0.179	0.180	0.180
	B_4^2	3.94(5)	4.03	4.01	3.97	4.01	4.00
	B_4^4	−3.24(5)	−3.10	−3.15	−3.00	−3.05	−3.05
Cs$^+$	B_4^0	0.169(5)	0.156	0.160	0.177	0.197	0.197
	B_4^2	3.73(5)	4.06	4.06	3.96	4.05	4.05
	B_4^4	−3.25(5)	−3.09	−3.13	−2.99	−3.19	−3.19
$\bar{B}_4'$			0.256(7)	0.255(7)	0.257(5)	0.240(8)	0.258(21)
$\bar{B}_4''$			[0]	−3.6(70)	[0]	43(16)	36(16)
R_0(Å)			[2.354]	[2.354]	[2.354]	[2.354]	2.252(35)
t_4			2.4(22)	3.4(29)	−5.6(8)	−7.2(9)	[10]
RMS deviation			0.164	0.159	0.144	0.128	0.127

with $t_4 = 10$, it is valid for a very narrow spread of ligand distances (about $\pm 0.8\%$ with respect to the mean distance $\bar{R} = 2.347$ Å) whereas the present set of systems shows a much greater distance variations ($\pm 2.6\%$ with $\bar{R} = 2.322$ Å).

Furthermore, we have purposely fixed the values of t_n in column (e) in tables 3 and 4 at those values obtained by Edgar and Newman (1975) for the single power-law form (3) while the reference distance R_0 is free to vary away from the host ligand distance. The results are such that the fitted values of the spin parameters in fits (d) and (e) are essentially identical, showing that the power-law exponent t_n can be fully absorbed in the parabolic form. It is also noted that we have attempted an alternative fit to substitute for the exponent 2 in the second term of equation (10) with an adjustable parameter, but the best fitted value is 2.4 ± 1.1 without any significant reduction in the RMS deviations. Another alternative is to try a double-power-law form as described by equation (2), but the contributing least-squares fit equations for the present sets of data are nearly ill-conditioned as the free parameters are highly correlated. Consequently, no unique or convergent values of parameters for (2) could be obtained and this problem may be overcome only if the physical system contains ligands spreading at much wider distances R_i.

4. Conclusions

The Kanzaki lattice statics method has been modified and adapted specifically for calculating the local distortions around the five orthorhombic Gd^{3+}–M^+ (M = Li, Na, K, Rb and Cs) complexes in CaF_2. Our lattice relaxation model is more reliable than Mott and Littleton's semidiscrete model used by Bijvank and Hartog (1980b) in three principal aspects: (i) no continuum approximation and mismatch problem embedded in the foundation of the model, (ii) higher accuracy for ionic shifts in the Gd^{3+}: K^+: CaF_2 complex as compared with ENDOR and ESEEM experiments, and (iii) much better description of the spin parameters of Gd^{3+} on using the calculated ligand positions in conjunction with the superposition model. As mentioned in section 1, there are various cancelling physical mechanisms contributing to the intrinsic spin parameters $\bar{B}_n(R)$ of Gd^{3+} and the overall effect would result in a local U-shaped extrema according to Newman and Urban (1975). The results of our present superposition model analysis (with local distortions) also empirically confirm the existence of such U-shaped extrema which can best be described by our parabolic form given in equation (10). The conventional power-law form (3) for $\bar{B}_n(R)$ which could not represent any cancelling effects was shown to be rather inadequate for greater ligand variation and the second term of our generalized form (10) also asserts the importance of the cancelling nature of various physical contributions to the ground state splitting of Gd^{3+}. In other words, our empirical data on the distance variation of the F^- ligand against the intrinsic parameters of Gd^{3+} should be very useful in filling in the details of *ab initio* calculations (e.g. Newman and Urban 1975, Pastusiak 1984, Siu 1990) of the major contributions based on existing or new physical mechanisms. They should also be useful in comparing such calculations with experimental results on the sign and magnitude of the zero-field splitting of Gd^{3+}, as well as their distance variation.

Acknowledgment

References

Bijvank E J and den Hartog H W 1980a *Phys. Rev.* B **22** 4121
—— 1980b *Phys. Rev.* B **22** 4133
Bijvank E J, den Hartog H W and Andriessen J 1977 *Phys. Rev.* B **16** 1008
Choy T L and Yeung Y Y 1990 *Phys. Status Solidi* b **161** K107
Cochran W 1971 *CRC Crit. Rev. Solid State Sci.* **2** 1
Drogendijk A C, Barkhuijsen H, de Beer R, van Ormondt D, Postma H and den Hartog H W 1987 *Hyperfine Interact.* **35** 1065
Edgar A and Newman D J 1975 *J. Phys. C: Solid State Phys.* **8** 4028
Elcombe M M and Pryor A W 1970 *J. Phys. C: Solid State Phys.* **3** 492
Kanzaki H 1957 *J. Phys. Chem. Solids* **2** 24
Lefferts A N, Bijvank E J and den Hartog H W 1978 *Phys. Rev.* B **17** 4214
Mott N F and Littleton M J 1938 *Trans. Faraday Soc.* **34** 485
Newman D J 1975 *J. Phys. C: Solid State Phys.* **8** 1862
Newman D J and Urban W 1975 *Adv. Phys.* **24** 793
Novak P and Vosika L 1983 *Czech. J. Phys.* B **33** 1134

Pastusiak W 1984 *Phys. Status Solidi* b **126** K77
Pryce M H L 1950 *Phys. Rev.* **80** 1107
Siu G G 1990 *J. Chem. Phys.* **92** 97
Yeung Y Y 1988 *J. Phys. C: Solid State Phys.* **21** L549
Yeung Y Y and Newman D J 1986 *J. Phys. C: Solid State Phys.* **19** 3877
—— 1987 *J. Chem. Phys.* **86** 6717
—— 1988 *J. Phys. C: Solid State Phys.* **21** 537